Inorg. Chem. **2004**, *43*, 7111–7119

Zirconium, Hafnium, and Tantalum Amide Silyl Complexes: Their Preparation and Conversion to Metallaheterocyclic Complexes via γ-Hydrogen Abstraction by Silyl Ligands

Xianghua Yu,[†] Siwei Bi,[‡] Ilia A. Guzei,[§] Zhenyang Lin,*[,‡] and Zi-Ling Xue*[,†]

Departments of Chemistry, The University of Tennessee, Knoxville, Tennessee 37996-1600, The Hong Kong University of Science and Technology, Clear Water Bay, Kowloon, Hong Kong, P. R. China, and The University of Wisconsin—Madison, Madison, Wisconsin 53706-1396

Received July 21, 2004

New transition metal silyl amide complexes $(Me_2N)_3Ta[N(SiMe_3)_2](SiPh_2Bu^t)$ (**1**) and $(Me_2N)M[N(SiMe_3)_2]_2(SiPh_2Bu^t)$ (M = Zr, **2a**, and Hf, **2b**) were found to undergo γ-H abstraction by the silyl ligands to give metallaheterocyclic complexes $(Me_2N)_3\overline{Ta(NSiMe_3SiMe_2CH_2)}$ (**3**) and $\{(Me_2N)[(Me_3Si)_2N]\overline{M(NSiMe_3SiMe_2CH_2)}\}_2$ (M = Zr, **4a**, and Hf, **4b**), respectively. The conversion of **1** to **3** follows first-order kinetics with $\Delta H^{\ddagger} = 23.6(1.6)$ kcal/mol and $\Delta S^{\ddagger} = 3(5)$ eu between 288 and 313 K. The formation of **4a** from $(Me_2N)Zr[N(SiMe_3)_2]_2Cl$ (**5a**) and $Li(THF)_2SiPh_2Bu^t$ (**6**) involves the formation of the intermediate **2a**, followed by γ-H abstraction. Kinetic studies of these consecutive reactions, a second-order reaction to give **2a** and then a first-order γ-H abstraction to give **4a**, were conducted by an analytical method and a numerical method. At 278 K, the rate constants k_1 and k_2 for the two consecutive reactions are $2.17(0.03) \times 10^{-3}$ M^{-1} s^{-1} and $5.80(0.15) \times 10^{-5}$ s^{-1} by the analytical method. The current work is a rare kinetic study of the A + B → C → D (+ E) consecutive reactions. Kinetic studies of the formation of a metallaheterocyclic moiety $\overline{M(NSiMe_3SiMe_2CH_2)}$ have, to our knowledge, not been reported. In addition, γ-H abstraction by a silyl ligand to give such a metallaheterocyclic moiety is new. Theoretical investigations of the γ-H abstraction by silyl ligands have been conducted by density functional theory calculations at the Becke3LYP (B3LYP) level, and they revealed that the formation of the metallacyclic complexes through γ-H abstraction is entropically driven. X-ray crystal structures of $(Me_2N)_3Ta[N(SiMe_3)_2](SiPh_2Bu^t)$ (**1**), $(Me_2N)Zr[N(SiMe_3)_2]_2Cl$ (**5a**), and $\{(Me_2N)[(Me_3Si)_2N]\overline{M(NSiMe_3SiMe_2CH_2)}\}_2$ (M = Zr, **4a**, and Hf, **4b**) are also reported.

Introduction

Transition-metal silyl complexes are of intense current interest.[1−3] d^0 silyl complexes free of cyclopentadienyl (Cp) ligands have been studied for their structures and reactivities.[1,3] Cp-free d^0 early transition metal complexes are often

* To whom correspondence should be addressed. E-mail: xue@utk.edu (Z.-L.X.), chzlin@ust.hk (Z.L.).
[†] The University of Tennessee.
[‡] The Hong Kong University of Science and Technology.
[§] The University of Wisconsin—Madison.

(1) (a) Tilley, T. D. In *The Silicon−Heteroatom Bond*; Patai, S., Rappoport, Z., Eds.; Wiley: New York, 1991; Chapters 9 and 10. (b) Eisen, M. S. In *The Chemistry of Organic Silicon Compounds*; Rappoport, Z., Apeloig, Y., Eds.; Wiley: New York, 1998; Vol. 2, Part 3, p 2037. (c) Harrod, J. F.; Mu, Y.; Samuel, E. *Polyhedron* **1991**, *10*, 1239. (d) Corey, J. Y.; Braddock-Wilking, J. *Chem. Rev.* **1999**, *99*, 175. (e) Tilley, T. D. *Acc. Chem. Res*. **1993**, *26*, 22. (f) Sharma, H. K.; Pannell, K. H. *Chem. Rev.* **1995**, *95*, 1351. (g) Schubert, U. *Transition Met. Chem.* **1991**, *16*, 136. (h) Xue, Z. *Comments Inorg. Chem*. **1996**, *18*, 223.

(2) See, e.g.: (a) Heyn, R. H.; Tilley, T. D. *Inorg. Chem.* **1990**, *29*, 4051. (b) Sadow, A. D.; Tilley, T. D. *J. Am. Chem. Soc.* **2003**, *125*, 9462. (b) Dioumaev, V. K.; Harrod, J. F. *Organometallics* **2000**, *19*, 583. (c) Dioumaev, V. K.; Yoo, B. R.; Procopio, L. J.; Carroll, P. J.; Berry, D. H. *J. Am. Chem. Soc.* **2003**, *125*, 8936. (d) Huhmann, J. L.; Corey, J. Y.; Rath, N. P. *J. Organomet. Chem*. **1997**, *533*, 61. (e) King, W. A.; Marks, T. J. *Inorg. Chim. Acta* **1995**, *229*, 343. (f) Banovetz, J. P.; Suzuki, H.; Waymouth, R. M. *Organometallics* **1993**, *12*, 4700. (g) Curtis, M. D.; Bell, L. G.; Butler, W. M. *Organometallics* **1985**, *4*, 701. (h) Jiang, Q.; Carroll, P. J.; Berry, D. H. *Organometallics* **1991**, *10*, 3648. (i) Arnold, J.; Shina, D. N.; Tilley, T. D.; Arif, A. M. *Organometallics* **1986**, *5*, 2037. (j) Ustinov, M. V.; Bravo-Zhivotoskii, D. A.; Kalikhman, I. D.; Vitkovskii, V. Yu.; Vyazankin, N. S.; Voronkov, M. G. *Organomet. Chem. U.S.S.R.* **1989**, *2*, 664. (k) Ovchinnikov, Yu. E.; Struchkov, Yu. T.; Ustinov, M. V.; Voronkov, M. G. *Russ. Chem. Bull.* **1993**, *8*, 1411. (l) Hengge, E.; Gspaltl, P.; Pinter, E. *J. Organomet. Chem*. **1996**, *521*, 145. (m) Campion, B. K.; Heyn, R. H.; Tilley, T. D. *Organometallics* **1993**, *12*, 2584.

10.1021/ic049023v CCC: $27.50
Published on Web 09/25/2004

highly electron deficient, and amide ligands such as $-NMe_2$ containing lone-pair electrons enhance the stability of these complexes through d−p π bonding.[2j,k,3e,k,4] Disilylamide ligand $-N(SiMe_3)_2$, as a bulkier and weaker p−d π bond donor than dialkylamide ligands,[5] often displays unique chemistry. For example, conversion of disilylamide ligands to the metallaheterocyclic moiety $\overline{M(NSiMe_3SiMe_2CH_2)}$ is known.[6] To our knowledge, γ-H activation of the $-N(SiMe_3)_2$ ligand by a silyl ligand to give a cyclic complex has not been reported. Here we report the preparation of amide silyl complexes $(Me_2N)_3Ta[N(SiMe_3)_2](SiPh_2Bu^t)$ (**1**) and $(Me_2N)M[N(SiMe_3)_2]_2(SiPh_2Bu^t)$ (M = Zr, **2a**, and Hf, **2b**) and their conversion to four-membered metallaheterocyclic complexes $(Me_2N)_3\overline{Ta(NSiMe_3SiMe_2CH_2)}$ (**3**) and $\{(Me_2N)[(Me_3Si)_2N]\overline{M(NSiMe_3SiMe_2CH_2)}\}_2$ (M = Zr, **4a**, and Hf, **4b**) through γ-H abstraction by the silyl ligands. The Zr and Hf silyl complexes **2a**,**b** were found to be too unstable to be isolated and were observed in-situ by ^{1}H NMR spectroscopy. The formation of the Zr four-membered ring complex **4a** from $(Me_2N)Zr[N(SiMe_3)_2]_2Cl$ (**5a**) and $Li(THF)_2SiPh_2Bu^t$ (**6**) follows consecutive reaction kinetics: second-order reaction to give **2a**, followed by first-order γ-H abstraction reaction to yield **4a**. Although there are standard procedures to study kinetics of two or three consecutive *first-order* reactions,[7] kinetic studies of a second-order reaction, followed by a first-order reaction, as observed here, are rare.[8] In addition, kinetic studies of the formation of metallaheterocyclic moiety $\overline{M(NSiMe_3SiMe_2CH_2)}$ have, to our knowledge, not been reported.[6] An analytical method has been developed in the current work for such consecutive reactions. Mathematic models by analytic methods are known to reveal physics and chemistry behind observed data and phenomena and are needed for benchmarking and validating numerical solutions and methods.[9] The kinetics of the consecutive reactions has been studied by both the analytical method developed in the current work and a numerical method. Our preparation of the new complexes, the analytical method for the consecutive reactions, kinetic studies of the formation of **3** and **4a**, and theoretical studies of the γ-H abstraction by silyl ligands are reported here.

Experimental Section

All manipulations were performed under a dry nitrogen atmosphere with the use of either a drybox or standard Schlenk techniques. All solvents were purified by distillation from potassium/benzophenone ketyl. Benzene-d_6, toluene-d_8, and THF-d_8 were dried over activated molecular sieves and stored under N_2. $TaCl_5$ (Strem) was used as purchased. $ZrCl_4$ and $HfCl_4$ (Strem) were freshly sublimed under vacuum. $Li(THF)_2SiPh_2Bu^t$ (**6**)[2m] and $(Me_2N)_3Ta[N(SiMe_3)_2]Cl$ (**7**)[6q] were prepared according to literature procedures. ^{1}H, ^{13}C{^{1}H}, and ^{29}Si{^{1}H} NMR spectra were recorded on a Bruker AMX-400 spectrometer and referenced to solvent (residual protons in the ^{1}H spectra). ^{29}Si chemical shifts were

(3) (a) Xue, Z.-L.; Li, L.-T.; Hoyt, L. K.; Diminnie, J. B.; Pollitte, J. L. *J. Am. Chem. Soc.* **1994**, *116*, 2169. (b) McAlexander, L. H.; Hung, M.; Li, L.-T.; Diminnie, J. B.; Xue, Z.-L.; Yap, G. P. A.; Rheingold, A. L. *Organometallics* **1996**, *15*, 5231. (c) Wu, Z.-Z.; McAlexander, L. H.; Diminnie, J. B.; Xue, Z.-L. *Organometallics* **1998**, *17*, 4853. (d) Li, L.-T.; Diminnie, J. B.; Liu, X.-Z.; Pollitte, J. L.; Xue, Z.-L. *Organometallics* **1996**, *15*, 3520. (e) Chen, T.-N.; Wu, Z.-Z.; Li, L.-T.; Sorasaenee, K. R.; Diminnie, J. B.; Pan, H.-J.; Guzei, I. A.; Rheingold, A. L.; Xue, Z.-L. *J. Am. Chem. Soc.* **1998**, *120*, 13519. (f) Wu, Z.-Z.; Diminnie, J. B.; Xue, Z.-L. *Inorg. Chem.* **1998**, *37*, 6366. (g) Choi, S.-H.; Lin, Z.-Y.; Xue, Z.-L. *Organometallics* **1999**, *18*, 5488. (h) Wu, Z.-Z.; Xue, Z.-L. *Organometallics* **2000**, *19*, 4191. (i) Wu, Z.-Z.; Diminnie, J. B.; Xue, Z.-L. *J. Am. Chem. Soc.* **1999**, *121*, 4300. (j) Wu, Z.-Z.; Diminnie, J. B.; Xue, Z.-L. *Organometallics* **1998**, *17*, 2917. (k) Wu, Z.-Z.; Cai, H.; Yu, X.-H.; Blanton, J. R.; Diminnie, J. B.; Pan, H.-J. Xue, Z.-L. *Organometallics* **2002**, *21*, 3973. (i) Yu, X.-H.; Cai, H.; Guzei, I. A.; Xue, Z.-L. *J. Am. Chem. Soc.* **2004**, *126*, 4472.

(4) (a) Lappert, M. F.; Power, P. P.; Sanger, A. R.; Srivastava, R. C. *Metal and Metalloid Amides*: Ellis Horwood: London, 1980. (b) Chisholm, M. H.; Rothwell, I. P. In *Comprehensive Coordination Chemistry*; Wilkinson, G., Gillard, R. D., McCleverty, J. A., Eds.; Pergamon: New York, 1987; Vol. 2.

(5) See, e.g.: (a) Bradley, D. C.; Hursthouse, M. B.; Abdul Malik, K. M.; Vuru, G. B. C. *Inorg. Chim. Acta* **1980**, *44*, L5. (b) Tilley, T. D.; Andersen, R. A.; Zalkin, A. *Inorg. Chem.* **1984**, *23*, 2271. (c) Hoffman, D. M.; Suh, S. *J. Chem. Soc., Chem. Commun.* **1993**, 714. (d) Avens, L. R.; Bott, S. G.; Clark, D. L.; Sattelberger, A. P.; Watkin, J. G.; Zwick, B. D. *Inorg. Chem.* **1994**, *33*, 2248. (e) Stewart, J. L.; Andersen, R. A. *New J. Chem.* **1995**, *19*, 587. (f) Duan, Z.-B.; Schmidt, M.; Young, V. G., Jr.; Xie, X.-B.; McCarley, R. E.; Verkade, J. G. *J. Am. Chem. Soc.* **1996**, *118*, 5302.

(6) (a) Berno, P.; Gambarotta, S. *Organometallics* **1995**, *14*, 2159. (b) Scoles, L.; Ruppa, K. B. P.; Gambarotta, S. *J. Am. Chem. Soc.* **1996**, *118*, 2529. (c) Dubois, L. H.; Zegarski, B. R.; Girolami, G. S. *J. Electrochem. Soc.* **1992**, *139*, 3603. (d) Lewkebandara, T. S.; Sheridan, P. H.; Heeg, M. J.; Rheingold, A. L.; Winter, C. H. *Inorg. Chem.* **1994**, *33*, 5879. (e) Beaudoin, M.; Scott, S. L. *Organometallics* **2001**, *20*, 237. (f) Cundari, T. R.; Morse, J. M., Jr. *Chem. Mater.* **1996**, *8*, 189. (g) Weiller, B. H. *J. Am. Chem. Soc.* **1996**, *118*, 4975. (h) Cale, T. S.; Chaara, M. B.; Raupp, G. B.; Raaijmakers, I. J. *Thin Solid Films* **1993**, *236*, 294. (i) Ossola, F.; Maury, F. *Chem. Vap. Deposition* **1997**, *3*, 137. (j) Bennett, C. R.; Bradley, D. C. *J. Chem. Soc., Chem. Commun.* **1974**, 29. (k) Simpson, S. J.; Andersen, R. A. *Inorg. Chem.* **1981**, *20*, 3627. (l) Bott, S. G. D.; Hoffman, M.; Rangarajan, S. P. *J. Chem. Soc., Dalton Trans.* **1996**, 1979. (m) Putzer, M. A.; Magull, J.; Goesmann, H.; Neumüller, B.; Dehnicke, K. *Chem. Ber.* **1996**, *129*, 1401. (n) Putzer, M. A.; Neumüller, B.; Dehnicke, K. *Z. Anorg. Allg. Chem.* **1998**, *624*, 1087. (o) Moore, M.; Gambarotta, S.; Bensimon, C. *Organometallics* **1997**, *16*, 1086. (p) Horton, A. D.; de With, J. *Chem. Commun.* **1996**, 1375. (q) Cai, H.; Yu, X.-H.; Chen, T.; Chen, X.-T.; You, X.-Z.; Xue, Z. *Can. J. Chem.* **2003**, *81*, 1398.

(7) (a) Espenson, J. H. *Chemical Kinetics and Reaction Mechanism*, 2nd Ed.; McGraw-Hill: New York, 1995; Chapter 4, pp 70−100. (b) Connors, K. A. *Chemical Kinetics. The Study of Reaction Rates in Solution*; VCH: New York, 1990; pp 66−77. (c) Benson, S. W. *The Foundations of Chemical Kinetics*; McGraw-Hill: New York, 1960; pp 54−55. (d) Wilkins, R. G. *Kinetics and Mechanism of Reactions of Transition Metal Complexes*, 2nd ed.; VCH: New York, 1991; Section 1.6.2, pp 18−23. (e) Steinfeld, J. I.; Francisco, J. S.; Hase, W. L. *Chemical Kinetics and Dynamics*, 2nd ed.; Prentice Hall: Upper Saddle River, NJ, 1999; Chapter 2, pp 22−86.

(8) Our searches of *Chemical Abstracts* (*SciFinder*) and *Science Citation Index* (*Web of Science*) showed two prior approaches for the 2X → Y → Z consecutive reactions: (a) Chien, J.-Y. *J. Am. Chem. Soc.* **1948**, *70*, 2256. Balandin, A. A.; Leibenson, L. S. *Dokl. Akad. Nauk SSSR, Ser. A* (*Proc. Acad. Sci. USSR, Ser. A*) **1943**, *39*, 22. (b) Capellos, C.; Bielski, B. H. J. *Kinetic Systems. Mathematical Description of Chemical Kinetics in Solutions*; Wiley: New York, 1972; pp 95−100. Matuska, N. J.; Bose, R. N. *Res. Chem. Intermed.* **1997**, *23*, 109. In the closed-form solution developed by Chien, Balandin, and Leibenson,[8a] the solution depends on the tabulated exponential integral (Jahnke, E.; Emde, F.; Lösch, F. *Tables of Higher Functions*, 6th ed.; McGraw-Hill: New York, 1960; pp 17−23). In this approach used *before* modern computers were available, families of concentrations vs $(1 + a_0k_1t)^{-1}$ curves were plotted for various kinetic schemes and compared with the concentration−time data for the intermediate Y or product Z. A match identified the kinetic scheme and may lead to additional rate constant estimates.[7b]

(9) (a) Eriksson, K.; Estep, D.; Hansbo, P.; Johnson, C. *Computational Differential Equations*; Cambridge University Press: Cambridge, Great Britain, 1996; p 7. (b) Riggs, J. B. *An Introduction to Numerical Methods for Chemical Engineers*; Texas Tech University Press: Lubbock, TX, 1988; pp 399−405.

referenced to $SiMe_4$. The formation of $HSiPh_2Bu^t$ in the conversions of **1** to **3**, **2a** to **4a**, and **2b** to **4b** was confirmed by comparisons with its standard NMR spectra. Elemental analyses were performed by Complete Analysis Laboratories Inc., Parsippany, NJ.

Preparation of $(Me_2N)_3Ta[N(SiMe_3)_2](SiPh_2Bu^t)$ (1). To a mixture of $(Me_2N)_3Ta[N(SiMe_3)_2]Cl$ (**7**, 0.640 g, 1.26 mmol) and $Li(THF)_2SiPh_2Bu^t$ (**6**, 0.480 g, 1.51 mmol, 20% excess) was added hexanes (30 mL) at −50 °C. The solution was warmed to room temperature and stirred for 4 h. The solution was then filtered, concentrated, and cooled at −35 °C overnight to give brown crystals of **1** (0.483 g, 0.735 mmol, 58.5% yield): ^{1}H NMR (benzene-d_6, 400.1 MHz, 15 °C) δ 7.82, 7.27 (m, C_6H_5), 3.17 (s, 18H, NMe_2), 1.23 (s, 9H, $SiPh_2CMe_3$), 0.11 [s, 18H, $N(SiMe_3)_2$]; $^{13}C\{^1H\}$ NMR (benzene-d_6, 100.0 MHz, 15 °C) δ 149.4, 138.8, 138.0, 137.4, 136.5 (C_6H_5), 48.9 (NMe_2), 31.7 ($SiPh_2CMe_3$), 26.2 ($SiPh_2CMe_3$), 5.8 [$N(SiMe_3)_2$]; $^{29}Si\{^1H\}$ NMR (benzene-d_6, 127.1 MHz, 10 °C) δ 62.7 ($SiPh_2Bu^t$), −2.18 [$N(SiMe_3)_2$]. Anal. Calcd for $C_{28}H_{55}N_4Si_3Ta$: C, 47.17; H, 7.78. Found: C, 46.95; H, 7.92.

Preparation of $(Me_2N)Zr[N(SiMe_3)_2]_2Cl$ (5a). A slurry of $ZrCl_4$ (4.00 g, 17.2 mmol) in THF (30 mL) was treated with 1 equiv of $LiNMe_2$ (0.876 g, 17.2 mmol) in THF at −30 °C. The reaction mixture was stirred overnight after the temperature was warmed to room temperature. A 2 equiv amount of $LiN(SiMe_3)_2$ (5.74 g, 34.3 mmol) in THF (30 mL) was added at −30 °C, and the mixture was stirred overnight at room temperature. All volatiles were removed in vacuo, and the product was extracted with hexanes (50 mL). The solution was filtered, concentrated, and cooled at −35 °C overnight to give colorless crystals of **5a** (7.21 g, 14.7 mmol, 85.3% yield): ^{1}H NMR (benzene-d_6, 400.0 MHz, 23 °C) δ 3.01 (s, 6H, NMe_2), 0.33 [s, 36H, $N(SiMe_3)_2$]; $^{13}C\{^1H\}$ NMR (benzene-d_6, 100.0 MHz, 23 °C) δ 45.1 (NMe_2), 4.7 [$N(SiMe_3)_2$]. Anal. Calcd for $C_{14}H_{42}N_3Si_4ClZr$: C, 34.21; H, 8.61. Found: C, 33.95; H, 8.57.

Preparation of $(Me_2N)Hf[N(SiMe_3)_2]_2Cl$ (5b). A slurry of $HfCl_4$ (5.00 g, 15.6 mmol) in THF (40 mL) was treated with 1 equiv of $LiNMe_2$ (0.797 g, 15.6 mmol) at −30 °C. The reaction mixture was then stirred overnight after it was warmed to room temperature. A 2 equiv amount of $LiN(SiMe_3)_2$ (5.22 g, 31.2 mmol) in THF (30 mL) was added at −30 °C, and the mixture was stirred overnight. All volatiles were removed in vacuo, and the product was extracted with hexanes (50 mL). The solution was filtered, concentrated, and cooled at −35 °C for 1 day to give colorless crystals of **5b** (7.42 g, 12.8 mmol, 82.2% yield): ^{1}H NMR (benzene-d_6, 400.0 MHz, 23 °C) δ 3.04 (s, 6H, NMe_2), 0.33 [s, 36H, $N(SiMe_3)_2$]; $^{13}C\{^1H\}$ NMR (benzene-d_6, 100.0 MHz, 23 °C) δ 44.0 (NMe_2), 5.0 [$N(SiMe_3)_2$]. Anal. Calcd for $C_{14}H_{42}N_3Si_4ClHf$: C, 29.05; H, 7.31. Found: C, 28.93; H, 7.47.

Preparation of $\{(Me_2N)[(Me_3Si)_2N]Zr(NSiMe_3SiMe_2CH_2)\}_2$ (4a). To a mixture of $(Me_2N)Zr[N(SiMe_3)_2]_2Cl$ (**5a**, 0.707 g, 1.44 mmol) and $Li(THF)_2SiPh_2Bu^t$ (**6**, 0.459 g, 1.44 mmol) was added toluene (30 mL) at −30 °C. The mixture was stirred for 4 h after the temperature was warmed to room temperature. Pentane (20 mL) was added after volatiles were removed in vacuo. The brown solution was filtered, concentrated, and cooled at −35 °C overnight to give colorless crystals of **4a** (0.451 g, 0.496 mmol, 68.9% yield): ^{1}H NMR (THF-d_8, 400.0 MHz, 23 °C) δ 2.99 (s, 6H, NMe_2), 0.30 (s, 3H, Si*Me*), 0.25 (s, 2H, $SiCH_2$), 0.22 [s, 18H, $N(SiMe_3)_2$], 0.20 (s, 3H, Si*Me*), 0.14 (s, 9H, $SiMe_3$); $^{13}C\{^1H\}$ NMR (THF-d_8, 100.0 MHz, 23 °C) δ 45.8 (NMe_2), 37.2 ($SiCH_2$), 5.7 (Si*Me*), 5.3 ($SiMe_3$), 5.2 [$N(SiMe_3)_2$], 4.9 (Si*Me*). In benzene-d_6 at 23 °C, the CH_2 resonance was not resolved in the ^{13}C NMR spectrum. When 2 equiv of THF was added into solution, the CH_2 peak at 37.3 ppm in ^{13}C NMR spectrum sharpened. Anal. Calcd for $C_{28}H_{82}N_6Si_8Zr_2$: C, 36.95; H, 9.08. Found: C, 36.73; H, 8.98.

Table 1. Rate Constants k for the Conversion of **1** to **3**[a]

T (K)	$(k \pm \delta k_{(ran)}) \times 10^5$ (s^{-1})
288 ± 1	2.98 ± 0.17
293 ± 1	5.84 ± 0.16
298 ± 1	11.9 ± 0.3
303 ± 1	24.50 ± 0.07
308 ± 1	47.7 ± 0.5
313 ± 1	83.1 ± 0.4

[a] The largest random uncertainty is $\delta k(\text{ran})/k = 0.17/2.98 = 5.7\%$. The total uncertainty of $\delta k/k = 7.6\%$ was calculated from $\delta k(\text{ran})/k = 5.7\%$ and estimated systematic uncertainty $\delta k(\text{sys})/k = 5\%$. The total uncertainty $\delta k/k$ and $\delta T = 1$ K were used in the calculations of uncertainties in the activation enthalpy $\Delta H^{\ddagger}$ and activation entropy $\Delta S^{\ddagger}$ by the error propagation formulas derived from the Eyring equation by Girolami and co-workers.[14]

Preparation of $\{(Me_2N)[(Me_3Si)_2N]Hf(NSiMe_3SiMe_2CH_2)\}_2$ (4b). A mixture of $(Me_2N)Hf[N(SiMe_3)_2]_2Cl$ (**5b**, 1.29 g, 2.23 mmol) and $Li(THF)_2SiPh_2Bu^t$ (**6**, 0.459 g, 2.24 mmol) was added toluene at −30 °C. The reaction mixture was stirred for 4 h after the mixture was warmed to room temperature. Pentane (20 mL) was added after all volatiles were removed in vacuo. The brown solution was filtered, concentrated, and cooled at −35 °C overnight to give colorless crystals of **4b** (0.766 g, 0.706 mmol, 63.3% yield): ^{1}H NMR (THF-d_8, 400.0 MHz, 23 °C) δ 3.01 (s, 6H, NMe_2), 0.25 (s, 2H, $SiCH_2$), 0.24 (s, 3H, Si*Me*), 0.23 (s, 3H, Si*Me*), 0.21 [18H, $N(SiMe_3)_2$], 0.14 (9H, $SiMe_3$); $^{13}C\{^1H\}$ NMR (THF-d_8, 100.0 MHz, 23 °C) δ 45.8 (NMe_2), 42.1 ($SiCH_2$), 5.5 (Si*Me*), 5.4 ($SiMe_3$), 5.3 [$N(SiMe_3)_2$], 4.8 (Si*Me*). Anal. Calcd for $C_{28}H_{82}N_6Si_8Hf_2$: C, 31.01; H, 7.62. Found: C, 30.83; H, 7.47.

Kinetic Study of the Conversion of $(Me_2N)_3Ta[N(SiMe_3)_2](SiPh_2Bu^t)$ (1) to 3. Complex **1** was mixed with an internal standard 4,4′-dimethylbiphenyl in a Young's NMR tube. The mixture was frozen in liquid nitrogen as soon as toluene-d_8 was added. For kinetics studies at 288−303 K, the NMR spectrometer was preset to the temperature, and the NMR tube was briefly thawed shortly before the NMR tube was inserted to the spectrometer. ^{1}H spectra at 288−303 K were recorded directly on the NMR spectrometer. For the kinetic studies at 308 and 313 K, the reaction was carried out in a heating circulation system. The solutions were then placed in a liquid nitrogen bath to quench the reaction, and the spectra were taken at 258 K. Rate constants derived from fitting of the data by first-order kinetics are given in Table 1.[10]

Kinetic Study of the Formation of $\{(Me_2N)[(Me_3Si)_2N]Zr(NSiMe_3SiMe_2CH_2)\}_2$ (4a) at 278 K. In a typical kinetic study of the formation of **4a**, $(Me_2N)Zr[N(SiMe_3)_2]_2Cl$ (**5a**) and $Li(THF)_2SiPh_2Bu^t$ (**6**) were mixed in a 1:1 ratio with an internal standard 4,4′-dimethylbiphenyl in a Young's NMR tube. The mixture was immediately frozen in liquid nitrogen after toluene-d_8 was added. The ^{1}H spectra were then taken at 278 K on a NMR spectrometer. In the first run, **5a** (36.9 mg, 0.0751 mmol), **6** (23.9 mg, 0.0751 mmol), and 4,4′-dimethylbiphenyl (11.2 mg, 0.0615 mmol) were mixed to give a solution of 0.558 mL. In the second run, **5a** (36.3 mg, 0.0738 mmol), **6** (23.5 mg, 0.0738 mmol), and 4,4′-dimethylbiphenyl (11.7 mg, 0.0642 mmol) were mixed to give a solution of 0.542 mL. The first step of the consecutive reactions, the formation of $(Me_2N)Zr[N(SiMe_3)_2]_2(SiPh_2Bu^t)$ (**2a**) from **5a** and **6** (Scheme 2), was found to follow second-order kinetics, and rate constants of the reaction were directly calculated from the plots of

(10) See Supporting Information for details.

$1/[LiSiPh_2Bu^t]$ vs *t*. The second step of the consecutive reactions, the conversion of **2a** to give cyclic **4a**, was found to follow first-order kinetics, as discussed below. Two different methods were employed to calculate the rate constant k_2 for the second step (Scheme 2): (1) fitting of the data by an analytical method directly derived from consecutive reactions—a second-order reaction followed by a first-order reaction; (2) a numerical method. The JMP program version 5.0.1 (SAS Institute Inc., Cary, NC) was used for data fitting and simulation by the analytical method. In the numerical method, the Gepasi program (version 3.30) was used, and the fitting method was conducted by the Levenberg−Marquardt method with maximum of 500 iterations and 0 tolerance.[11]

Determination of X-ray Crystal Structures of $(Me_2N)_3Ta[N(SiMe_3)_2](SiPh_2Bu^t)$ (1), $(Me_2N)Zr[N(SiMe_3)_2]_2Cl$ (5a), and $\{(Me_2N)[(Me_3Si)_2N]M(NSiMe_3SiMe_2CH_2)\}_2$ (M = Zr, 4a, and Hf, 4b). The data for the crystal structures of these complexes were collected on a Bruker AXS Smart 1000 X-ray diffractometer with Mo radiation, equipped with a CCD area detector and fitted with an upgraded Nicolet LT-2 low-temperature device. Suitable crystals were coated with paratone oil (Exxon) and mounted on a hairloop under a stream of nitrogen gas at 173(2) K. The structure of **5a** was solved by Patterson method while the others were solved by direct methods. In all cases the non-hydrogen atoms were refined with anisotropic displacement coefficients. All hydrogen atoms were included in the structure factor calculation at idealized positions and were allowed to ride on the neighboring atoms with relative isotropic displacement coefficients. Empirical absorption correction was performed with SADABS.[12a] All calculations were performed using SHELXTL (version 5.1) proprietary software package.[12b]

Computation Details. Density functional theory calculations at the Becke3LYP (B3LYP) level have been used to perform the geometry optimizations for reactants, transition states, and products studied here. Frequency calculations at the same level of theory have also been performed to identify all stationary points as minima (zero imaginary frequency) or transition states (one imaginary frequency). The effective core potentials (ECPs) of Hay and Wadt with double-ζ valence basis set (LanL2DZ)[13a] were used to describe Ta and Si. For all other atoms, the standard 6-31G basis set was used. Polarization functions have been added for Si [$\zeta(d) = 0.262$] and for the H atom [$\zeta(p) = 1.1$] involved in the γ-H abstraction process. To examine the basis set dependence, we also performed single-point energy calculations with a better basis set. In the better basis set, instead of 6-31G, 6-31G** was used for C, N, and H atoms. With the smaller basis set, the relative energies for **A**, **TS**, and **B** are 0.0, 36.5, and −1.5 kcal/mol, respectively. With the better basis set, the relative energies for **A**, **TS**, and **B** are 0.0, 36.0, and −1.5 kcal/mol, respectively. These additional calculations suggest that the basis set used is appropriate. Here, **A** and **B** are the model complexes of **1** and **3**, respectively. Their structural details can be found in the section Computational Studies of the γ-H Abstraction Process. All calculations were performed with the use of the Gaussian 98 package[13b] on Silicon Graphics Indigo workstations and PC Pentium IV computers.

Scheme 1. Preparation of **1** and **3**

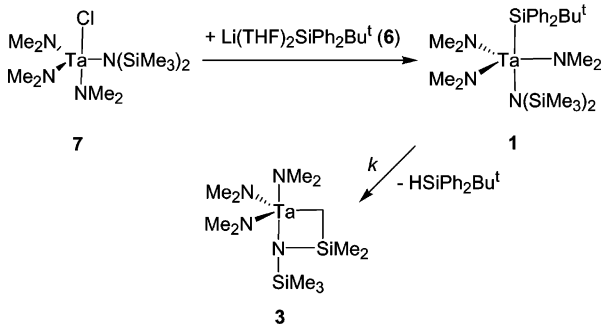

Results and Discussion

Synthesis of Ta Amide Silyl Complex $(Me_2N)_3Ta[N(SiMe_3)_2](SiPh_2Bu^t)$ (1) and the Kinetic Study of Its Conversion to Metallaheterocycle Complex $(Me_2N)_3Ta(NSiMe_3SiMe_2CH_2)$ (3). Treatment of $(Me_2N)_3Ta[N(SiMe_3)_2]Cl$ (**7**) with 1 equiv of $Li(THF)_2SiPh_2Bu^t$ (**6**) leads first to the silyl complex **1** (Scheme 1). **1** was found to be unstable and to convert to the metallaheterocycle complex **3** through a first-order kinetic process to be discussed below. **3** was reported earlier and prepared by either the reaction of **7** with 1 equiv of $LiN(SiMe_3)_2$ or the reaction of $Ta(NMe_2)_3Cl_2$ with 2 equiv of $LiN(SiMe_3)_2$.[6q] In the current formation of **3** from **1**, the silyl ligand abstracts a γ-H atom from the $-N(SiMe_3)_2$ ligand, giving silane $HSiPh_2Bu^t$ and the $-CH_2-Ta$ moiety in a four-membered cyclic structure. NMR spectra reveal a Berry pesudorotation process in **1**.[10] The peaks of the $-SiPh_2Bu^t$ and the $-N(SiMe_3)_2$ ligands in the ^1H NMR spectra of **1** split into two sets of peaks when the temperature was cooled below the coalescence temperature of 213 K.

The kinetics of the conversion of **1** to **3** was studied between 288 and 313 K.[10] A plot by the Eyring equation (Figure 1) gives activation parameters $\Delta H^{\ddagger} = 23.6(1.6)$ kcal/mol and $\Delta S^{\ddagger} = 3(5)$ eu. The activation enthalpy $\Delta H^{\ddagger}$ is in the range observed for other reactions involving C−H bond cleavage. The activation entropy $\Delta S^{\ddagger}$ is small for this γ-H abstraction process.

Synthesis and Characterization of Metallaheterocycle Complexes $\{(Me_2N)[(Me_3Si)_2N]M(NSiMe_3SiMe_2CH_2)\}_2$ (M = Zr, 4a, and Hf, 4b). NMR spectra of the reaction of **5a** with $Li(THF)_2SiPh_2Bu^t$ (**6**) were found to slowly give a set of new peaks, which were assigned to the silyl complex $(Me_2N)Zr[N(SiMe_3)_2]_2(SiPh_2Bu^t)$ (**2a**). Subsequently two new sets of NMR peaks, identified to be those of the metallaheterocycle complex **4a** and $HSiPh_2Bu^t$, respectively,

(11) (a) Gepasi 3.30, 2002 (http://www.gepasi.org/). (b) Mendes, P. *Comput. Appl. Biosci.* **1993**, *9*, 563. (c) Mendes, P. *Trends Biochem. Sci.* **1997**, *22*, 361.

(12) (a) Sheldrick, G. M. *SADABS, A Program for Empirical Absorption Correction of Area Detector Data*; University of Göttingen: Göttingen, Germany, 2000. (b) Sheldrick, G. M. *SHELXL-97, A Program for the Refinement of Crystal Structures*; University of Göttingen: Göttingen, Germany, 1997.

(13) (a) Hay, P. J.; Wadt, W. R. *J. Chem. Phys.* **1985**, *82*, 299. (b) Frisch, M. J.; Trucks, G. W.; Schlegel, H. B.; Scuseria, G. E.; Robb, M. A.; Cheeseman, J. R.; Zakrzewski, V. G.; Montgomery, J. A., Jr.; Stratmann, R. E.; Burant, J. C.; Dapprich, S.; Millam, J. M.; Daniels, A. D.; Kudin, K. N.; Strain, M. C.; Farkas, O.; Tomasi, J.; Barone, V.; Cossi, M.; Cammi, R.; Mennucci, B.; Pomelli, C.; Adamo, C.; Clifford, S.; Ochterski, J.; Petersson, G. A.; Ayala, P. Y.; Cui, Q.; Morokuma, K.; Malick, D. K.; Rabuck, A. D.; Raghavachari, K.; Foresman, J. B.; Cioslowski, J.; Ortiz, J. V.; Baboul, A. G.; Stefanov, B. B.; Liu, G.; Liashenko, A.; Piskorz, P.; Komaromi, I.; Gomperts, R.; Martin, R. L.; Fox, D. J.; Keith, T.; Al-Laham, M. A.; Peng, C. Y.; Nanayakkara, A.; Challacombe, M.; Gill, P. M. W.; Johnson, B.; Chen, W.; Wong, M. W.; Andres, J. L.; Gonzalez, C.; Head-Gordon, M.; Replogle, E. S.; Pople, J. A. *Gaussian 98*, (revision A.9); Gaussian, Inc.: Pittsburgh, PA, 1998.

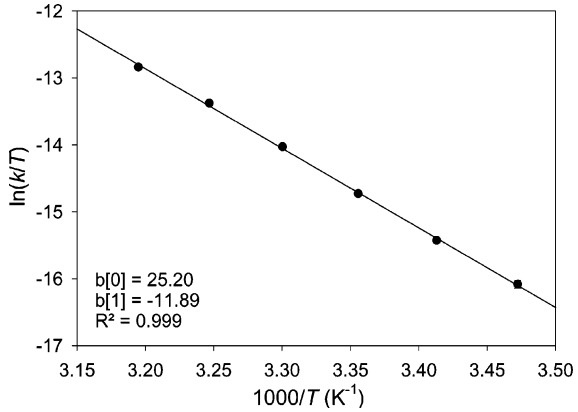

Figure 1. Eyring plot of the conversion of **1** to **3**.

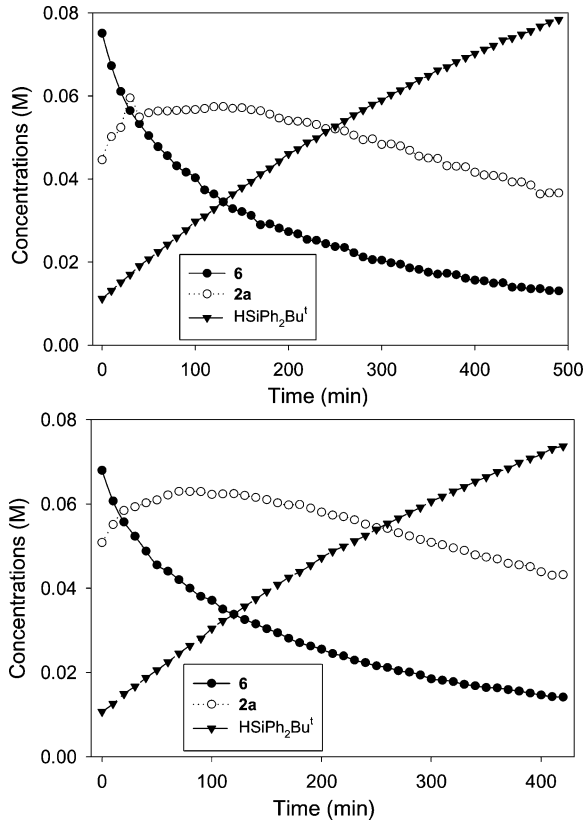

Figure 2. Kinetic plots of the formation of **4a** in Scheme 2 in the two runs at 278 K.

appeared and grew slowly. These observations suggest that **2a** is unstable and, as an intermediate, it converts to **4a** and $HSiPh_2Bu^t$. The changes of concentrations of **6**, **2a**, and the product $HSiPh_2Bu^t$ vs time are shown in Figure 2. The concentration of **2a** reaches its maximum and then decreases. The conversion of **2a** to the metallaheterocycle complex **4a** and $HSiPh_2Bu^t$ is a γ-H abstraction process from the $-N(SiMe_3)_2$ ligand by the silyl ligand. In the reaction of **5b** with $Li(THF)_2SiPh_2Bu^t$ (**6**), a similar conversion gives the metallaheterocycle complex **4b**. ^{1}H-coupled ^{13}C NMR spectra of **4a**,**b** confirmed the presence of the $-CH_2-$ moiety.

Kinetics of Consecutive Reactions Involving a Second-Order Reaction as the First Step. The first step in the consecutive reactions in Scheme 2 to give $(Me_2N)Zr[N(SiMe_3)_2]_2(SiPh_2Bu^t)$ (**2a**) was found to follow second-

Scheme 2. Preparation of **4a,b**[a]

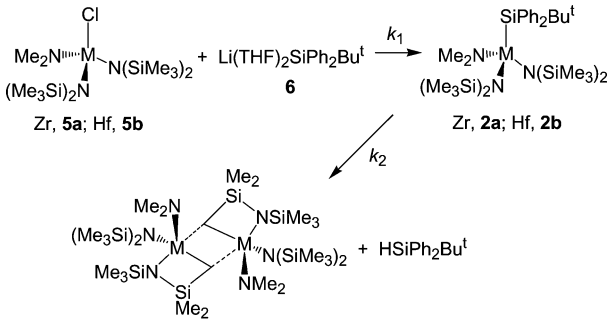

[a] k_1 and k_2 are the rate constants of the conversions of **5a** to **2a** and **2a** to **4a**, respectively.

order kinetics, and its rate constant k_1 could be obtained directly from the following integrated rate law: $1/[\mathbf{6}] - 1/[\mathbf{6}]_0 = k_1t$. The second step of the consecutive reactions, the formation of cyclic **4a** from **2a**, follows first-order kinetics. Two different methods were employed to calculate the rate constant k_2 for the second step (Scheme 2): (1) fitting of the data by an analytical method directly derived from consecutive reactions—a second-order reaction followed by a first-order reaction; (2) a numerical method. Kinetic studies by these methods are discussed here.

(a) Analytical Method. There have been few kinetic studies of the A + B → C → D (+ E) consecutive reactions involving a second-order reaction, followed by a first-order reaction.[8,15] We thus decided to derive the kinetic formula for such consecutive reactions. From eq 1

$$\mathbf{5a} + \mathbf{6} \xrightarrow{k_1} \mathbf{2a} \xrightarrow{k_2} \mathbf{4a} + HSiPh_2Bu^t$$

$t = 0$	B_0	B_0	0	0	0
$t = t$	B	B	C	D	D

$B-D$ are concentrations of **5a** (and **6**), **2a**, and **4a** (and $HSiPh_2Bu^t$), respectively. The formation of **2a** follows standard second-order kinetics. Thus, the integrated rate law is

$$1/B = k_1t + 1/B_0 \quad B = B_0/(k_1tB_0 + 1) \tag{2}$$

Fitting $1/B$ (i.e., $1/[\mathbf{6}]$) vs t by eq 2 thus gives the values of k_1. From eq 1, C, the concentration of the intermediate **2a** follows eq 3.

$$\frac{dC}{dt} = k_1B^2 - k_2C \quad \frac{dC}{dt} + k_2C = \frac{B_0{}^2k_1}{(B_0k_1t + 1)^2} \tag{3}$$

This is a $dy/dt + ay = Q$ type differential equation. The solution of such an equation is given in eq 4, and the details

(14) Morse, P. M.; Spencer, M. D.; Wilson, S. R.; Girolami, G. S. *Organometallics* **1994**, *13*, 1646.

(15) Pseudo-first-order approximations for the second-order step in consecutive reactions A + B → C → decompositions have been used to simplify the calculations. See, e.g.: Grimley, E.; Gordon, G. *J. Phys. Chem.* **1973**, *77*, 973.

Table 2. Crystallographic Data

	1	5a	4a	4b
formula	$C_{24}H_{55}N_4Si_3Ta$	$C_{14}H_{42}ClN_3Si_4Zr$	$C_{28}H_{82}N_6Si_8Zr_2$	$C_{28}H_{82}N_6Si_8Hf_2$
fw	712.98	491.52	910.13	1084.67
temp (K)	173(2)	173(2)	173(2)	173(2)
cryst system	monoclinic	monoclinic	triclinic	triclinic
space group	$P2_1/c$	$P2_1/c$	$P\bar{1}$	$P\bar{1}$
a (Å)	9.771(3)	10.229(3)	10.172(6)	10.151(4)
b (Å)	33.042(8)	29.358(8)	14.421(9)	14.368(5)
c (Å)	12.751(3)	18.166(5)	18.947(12)	18.921(7)
α (deg)	90	90	105.425(10)	105.330(6)
β (deg)	124.894(15)	105.498(5)	99.529(10)	99.331(6)
γ (deg)	90	90	105.110(10)	105.157(6)
V (Å^3)	3376.6(15)	5257(3)	2503(3)	2488.2(16)
Z	4	8	2	2
D(calcd) (g/cm^3)	1.403	1.242	1.208	1.448
μ (mm^{-1})	3.384	0.705	0.632	4.386
F(000)	1464	2080	968	1096
θ range (deg)	2.04−28.34	1.35−28.43	1.15−28.61	1.61−22.55
completeness (%)	96.3	97.2	92.2	99.3
no. of unique reflcns	8104	12873	11837	6503
no. of params varied	380	443	439	423
R indices[a] (R_wF^2)	0.0261 (0.0560)	0.0535 (0.1160)	0.0346 (0.0775)	0.0331 (0.0789)
goodness-of-fit on F^2	1.198	1.022	0.967	0.848

[a] $R = \Sigma||F_o| - |F_c||/\Sigma|F_o|$; $R_w = (\Sigma[w(F_o^2 - F_c^2)^2]/\Sigma[w(F_o^2)^2])^{1/2}$.

of the solution are given in the Supporting Information.[10]

$$y = e^{-at}\int e^{at}Q\,dt + Ke^{-at} \quad (4)$$

In the current case, the solution to eq 3 is thus

$$C = e^{-k_2t}\int_0^t e^{k_2t}\frac{k_1{B_0}^2}{(B_0k_1t+1)^2}\,dt = k_1{B_0}^2e^{-k_2t}\int_0^t\frac{e^{k_2t}}{(B_0k_1t+1)^2}\,dt \quad (5)$$

Using the Taylor expansion and integrating eq 5 gives eq 6 as an infinite series. This series is convergent as the ratio test confirmed.[10,16]

$$C = B_0e^{-k_2t}\frac{B_0}{k_1B_0t+1} + \frac{k_2}{k_1}e^{-(k_2t+(k_2/k_1B_0))}\ln(k_1B_0t+1) + \frac{{k_2}^2t}{k_1}e^{-(k_2t+(k_2/k_1B_0))}$$

$$+\frac{k_2}{4k_1}\left({k_2}^2t^2+\frac{2{k_2}^2}{k_1B_0}t\right)e^{-(k_2t+(k_2/k_1B_0))} + \frac{k_2}{18k_1}\left[\left(k_2t+\frac{k_2}{k_1B_0}\right)^3-\left(\frac{k_2}{k_1B_0}\right)^3\right]e^{-(k_2t+(k_2/k_1B_0))}$$

$$+\frac{k_2}{96k_1}\left[\left(k_2t+\frac{k_2}{k_1B_0}\right)^4-\left(\frac{k_2}{k_1B_0}\right)^4\right]e^{-(k_2t+(k_2/k_1B_0))}+\ldots \quad (6)$$

In the current work, kinetic studies were conducted at 278 K. Plots of concentrations of **6**, **2a**, and $HSiPh_2Bu^t$ ($B-D$, respectively) vs t are given in Figure 2. Fitting of eq 2 gives the rate constant $k_1 = 2.17(0.03) \times 10^{-3}$ M^{-1} s^{-1} for the first step in eq 1. The first 7 terms in eq 6 and values of k_1 and B_0 were used in the fitting by the JMP program (version 5.0.1) to give the rate constant $k_2 = 5.80(0.15) \times 10^{-5}$ s^{-1} for the second step in eq 1. The value of k_2 by this analytical method was then compared with that derived by a numerical method, which is discussed below.

(b) Numerical Method. In this approach, the differential equation eq 3 was solved to give k_2 by a numerical method using the rate constant k_1 derived from fitting B by eq 2. The Gepasi program (version 3.30)[11] was used in the studies to give $k_1 = 1.89(0.02) \times 10^{-3}$ M^{-1} s^{-1} and $k_2 = 5.32(0.20) \times 10^{-5}$ s^{-1}. Both values are close to those calculated by the analytical method.

The rate constant k_2 of γ-H abstraction by a silyl ligand to give the Zr cyclic complex **4a** at 278 K, the second step in Scheme 2, is similar to $k = 2.98(0.17) \times 10^{-5}$ s^{-1} at 288 K for the similar reaction in Scheme 1 to give the Ta cyclic complex **3**. As discussed below, theoretical studies show that the formation of the metallacyclic complexes through γ-H abstraction is entropically driven.

Molecular Structures of $(Me_2N)_3Ta[N(SiMe_3)_2](SiPh_2Bu^t)$ (1), $(Me_2N)Zr[N(SiMe_3)_2]_2Cl$ (5a), and $\{(Me_2N)[(Me_3Si)_2N]M(NSiMe_3SiMe_2CH_2)\}_2$ (M = Zr, 4a, and Hf, 4b). Crystal data for these complexes are given in Table 2. The crystal structure of **1** (Figure 3) showed a distorted trigonal bipyramidal configuration with the $-SiPh_2Bu^t$ and the $-N(SiMe_3)_2$ ligands in the axial positions and three $-NMe_2$ ligands in the equatorial positions. The equatorial $-NMe_2$ ligands are slightly tilted toward the $-SiPh_2Bu^t$ ligand, although the $-SiPh_2Bu^t$ ligand is sterically more demanding than the $-N(SiMe_3)_2$ ligand. This is perhaps a result of the d−p π bonding between Ta and the $-N(SiMe_3)_2$ ligand, leading to a shorter, stronger Ta(1)−N(4) bond and pushing the equatorial ligands away. The N(1)−Ta(1)−N(3) angle [142.11(10)°] is close to that [157.24(7)°] of N(4)−Ta(1)−Si(1). The NMR spectra of **1** indicate that the silyl $-SiPh_2Bu^t$ and amide $-N(SiMe_3)_2$ ligands are involved in a Berry pseudorotation process as discussed earlier. For the two $-SiMe_3$ groups in the $-N(SiMe_3)_2$ ligand, the Ta(1)···C(7)

(16) Arfken, G. *Mathematical Methods for Physicists*, 3rd ed.; Academic Press: Orlando, FL, 1985; pp 282−283.

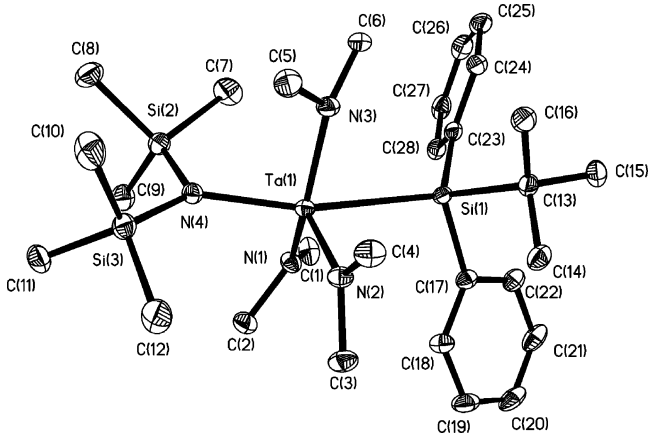

Figure 3. Molecular drawing of **1** showing 30% probability thermal ellipsoids. Selected bond distances (Å) and angles (deg): Ta(1)−N(1) 1.987(2), Ta(1)−N(4) 2.073(2), Ta(1)−Si(1) 2.9164(10); N(4)−Ta(1)−Si(1) 157.24(7), N(2)−Ta(1)−N(3) 105.21(10), N(1)−Ta(1)−N(2) 108.96(10), N(1)−Ta(1)−N(3) 142.11(10).

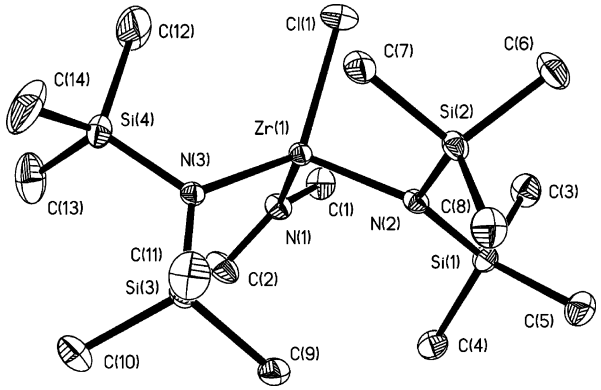

Figure 4. Molecular drawing of **5a** showing 30% probability thermal ellipsoids. Selected bond distances (Å) and angles (deg): Zr(1)−N(1) 2.024(3), Zr(1)−N(2) 2.056(3), Zr(1)−Cl(1) 2.4321(14); N(1)−Zr(1)−N(2) 107.70(14), N(1)−Zr(1)−N(3) 100.84(14), N(2)−Zr(1)−N(3) 114.26(13), N(1)−Zr(1)−Cl(1) 100.63(11), N(2)−Zr(1)−Cl(1) 101.55(10), N(3)−Zr(1)−Cl(1) 129.57(10).

and Ta(1)···Si(2) distances of 3.37 and 3.21 Å are shorter than the Ta(1)···C(12) and Ta(1)···Si(3) distances of 3.89 and 3.47 Å, respectively. The Si(2)−N(4)−Ta(1) bond angle of 113.90(12)° is significantly smaller than that of Si(3)−N(4)−Ta(1) [130.55(13)°]. These observations suggest agostic $Si_\beta-C_\gamma$ interaction[17] in the Ta−N(4)−Si(2)−C(7) moiety.

The structure of **5a** adopts a distorted tetrahedral configuration (Figure 4). The steric shielding of the two bulky $-N(SiMe_3)_2$ ligands prevents dimerization of this complex, as observed in $[Zr(NMe_2)_3(Cl)]_2(THF)$.[18] Except for the N(3)−Zr(1)−Cl(1) angle, other angles around the Zr atom in **5a** are close to the tetrahedron angle of 109.5°. The Zr(1)···C(7) and Zr(1)···Si(2) distances of 3.06 and 3.13 Å are significantly shorter than other Zr(1)···C (3.30−3.96 Å)

(17) (a) Koga, N.; Morokuma, K. *J. Am. Chem. Soc.* **1988**, *110*, 108. (b) Eisch, J. J.; Piotrowski, A. M.; Brownstein, S. K.; Gabe, E. J.; Lee, F. L. *J. Am. Chem. Soc.* **1985**, *107*, 7219. (c) Jeske, G.; Schock, L. E.; Swepston, P. N.; Schumann, H.; Marks, T. J. *J. Am. Chem. Soc.* **1985**, *107*, 8103. (d) Den Haan, K. H.; De Boer, J. L.; Teuben, J. H.; Spek, A. L.; Kojic-Prodic, B.; Hays, G. R.; Huis, R. *Organometallics* **1986**, *5*, 1726.

(18) Wu, Z.-Z.; Diminnie, J. B.; Xue, Z.-L. *Inorg. Chem.* **1998**, *37*, 2570.

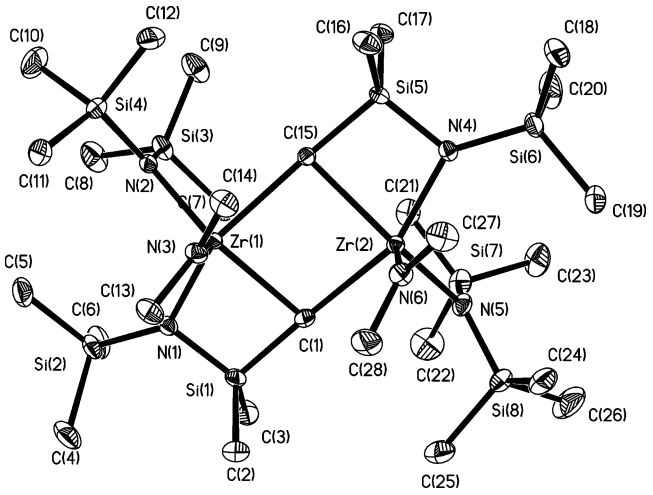

Figure 5. Molecular drawing of **4a** showing 30% probability thermal ellipsoids. Selected bond distances (Å) and angles (deg): Zr(1)−N(1) 2.096(2), Zr(1)−N(2) 2.128(2), Zr(1)−N(3) 2.018(2), Zr(1)−C(1) 2.467(3), Zr(1)−C(15) 2.471(3), Zr(2)−C(1) 2.474(3), Zr(2)−C(15) 2.474(3), Si(1)−C(1) 1.870(3), Si(1)−N(1) 1.731(3); N(1)−Zr(1)−C(1) 74.43(10), Si(1)−N(1)−Zr(1) 99.28(11), N(1)−Si(1)−C(1) 100.76(13), Si(1)−C(1)−Zr(1), 83.65(12), Zr(1)−C(1)−Zr(2) 93.11(11), C(1)−Zr(1)−C(15) 82.92(10).

Chart 1

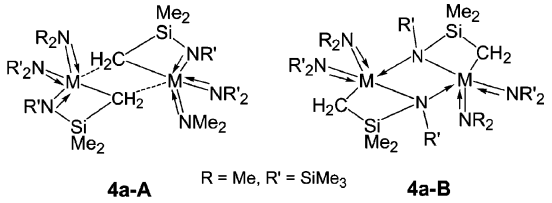

and Zr···Si (3.24−3.41 Å) distances, respectively. The Si(2)−N(2)−Zr(1) and N(2)−Si(2)−C(7) bond angles of 110.29(17) and 108.22(19)° are smaller than those of Si(1)−N(2)−Zr(1) [126.94(19)°] and N(2)−Si(1)−C(4) [111.95(19)°]. These observations suggest agostic $Si_\beta-C_\gamma$ interaction between Zr(1) and the Zr−N(2)−Si(2)−C(7) moiety. The Zr(1)···C(12) and Zr(1)···Si(4) distances of 3.30 and 3.24 Å are also shorter than the Zr···C(9) (3.66 Å) and Zr···Si(3) (3.40 Å) distances, respectively, suggesting agostic $Si_\beta-C_\gamma$ interaction in the Zr−N(3)−Si(4)−C(12) moiety as well, although the shortenings are not as significant as in the Zr−N(2)−Si(2)−C(7) moiety.

The Zr and Hf complexes **4a**,**b** are isomorphous. The structures of **4a**,**b** are shown in Figure 5 and the Supporting Information,[10] respectively. Electron deficiency and open coordination sphere lead to dimerization of the monomer "$(Me_2N)[(Me_3Si)_2N]M(NSiMe_3SiMe_2CH_2)$" in the solid state. It is interesting to note that the dimerization is achieved through the bridging $-CH_2-$ moiety rather than an amide ligand which often donates its lone-pair electrons to bridge with another metal atom.[4] If the terminal amide ligands fully donate their lone-pair electrons to the metal atoms through the p−d π bonds in the structures of **4a**,**b** so that there are 14e in the valence shells for each metal atom, the 3-center−2-electron bonding in the $-CH_2-$ bridges in **4a-A** in Chart 1 is expected to further alleviate electron deficiency in these complexes. In other words, a structure with bridging amide ligands (**4a-B**, Chart 1) would not take the advantage of the

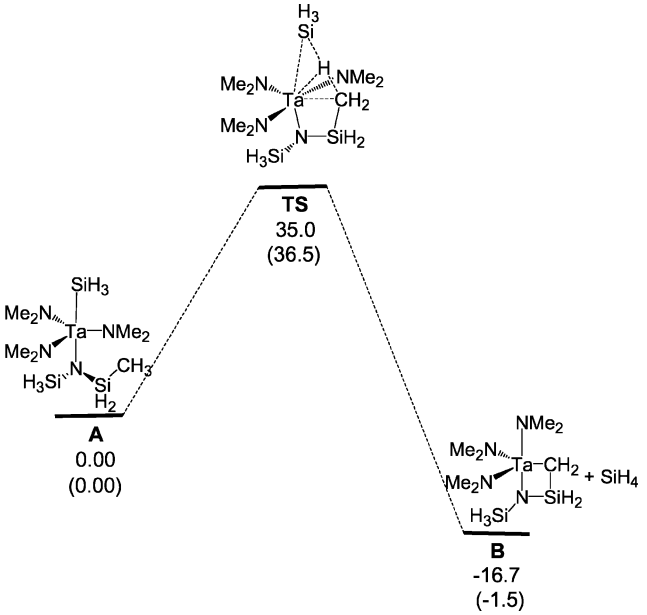

Figure 6. Potential energy profile for the γ-H abstraction process. Relative free energies (in kcal/mol) are given together with the relative energies (the values in parentheses).

3-center−2-electron bonding and is perhaps less preferred. In the structures of **4a**,**b**, the three cycles defined by N(1)−M(1)−C(1)−Si(1), M(1)−C(15)−M(2)−C(1), and C(15)−Si(5)−N(4)−M(2), respectively, are almost coplanar. The Zr(1)···C(7) and Zr(1)···Si(3) distances of 3.16 and 3.22 Å are shorter than those of Zr(1)···C(11) (3.98 Å) and Zr(1)−Si(4) (3.44 Å). The Si(3)−N(2)−Zr(1) and N(2)−Si(3)−C(7) bond angles of 113.06(12) and 108.47(14)° are both smaller than those of Si(4)−N(2)−Zr(1) [125.18(13)°] and N(2)−Si(4)−C(11) [113.99(13)°], respectively. These observations suggest agostic $Si_\beta-C_\gamma$ interaction in **4a** as well.

Computational Studies of the γ-H Abstraction Process. Kinetic studies discussed above show that the conversion from **1** to the metallacyclic complex **3** (Scheme 1) is a first-order reaction, suggesting that the γ-H abstraction is an intramolecular process. To understand how **1** undergoes the γ-H abstraction, we carried out theoretical studies with the aid of B3LYP density functional theory calculations.

Figure 6 shows the potential energy profile calculated for the conversion of complex **A**, a model complex of **1**, to complex **B**, a model complex of **3**. The activation free energy is calculated to be 35.0 kcal/mol. The activation energy (36.5 kcal/mol) differs only slightly from the activation free energy because the reaction is an intramolecular process. The activation free energy is at the lower end of those reported for γ-H abstraction mediated by group 4 transition metal complexes.[19] The calculated activation energy is, however, much greater than the experimentally measured $\Delta H^{\ddagger}$ value, likely due to the gas-phase model employed in our calculations. The reaction energy is calculated to be −1.5 kcal/mol while the reaction free energy is −16.7 kcal/mol, indicating that the γ-H abstraction is entropically driven. This result is consistent with early experimental findings that the entropy contribution is crucial in the formation of actinacyclobutanes through γ-H abstraction in complexes of the type $Cp_2Th(CH_2CMe_3)_2$.[20]

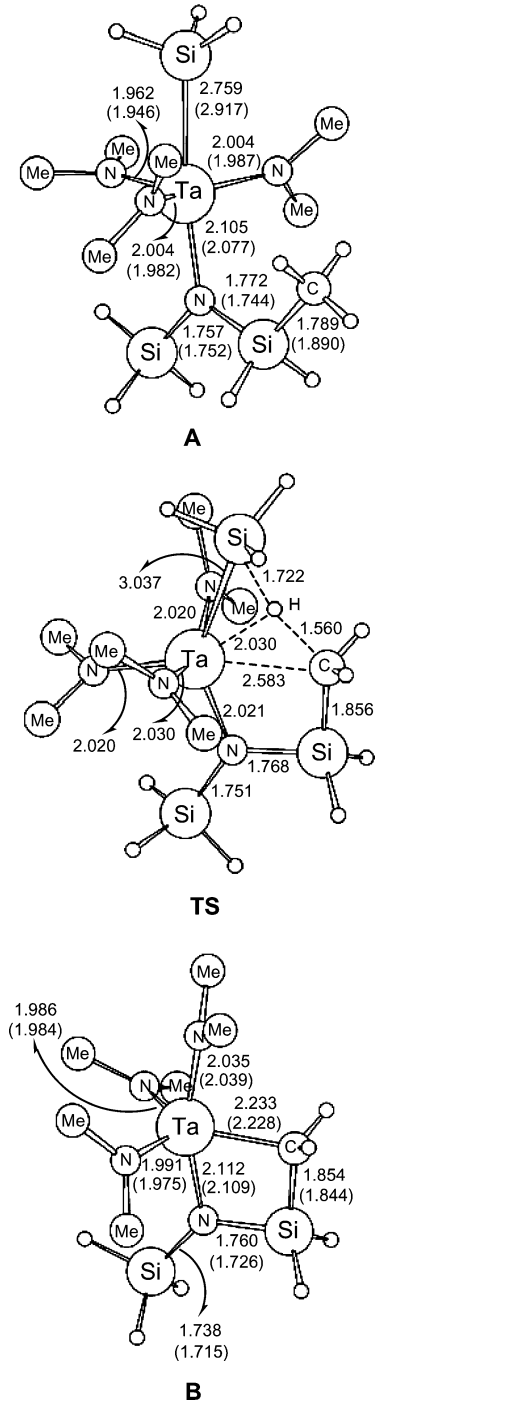

Figure 7. B3LYP/LANL2DZ-optimized structures for species shown in Figure 6. Selected bond distances (Å) calculated for the species are given. The values in parentheses were taken from the X-ray crystal structures of **1** and **3**. For the purpose of clarity, the H atoms of some methyl groups are omitted.

The calculated structures of model complexes **A** and **B** (Figure 7) reproduce well the experimental structures of **1**

(19) (a) Wu, Y.-D.; Peng, Z.-H.; Chan, K. W. K.; Liu, X.; Tuinman, A. A.; Xue, Z. *Organometallics* **1999**, *18*, 2081. (b) Wu, Y.-D.; Peng, Z.-H.; Xue, Z. *J. Am. Chem. Soc.* **1996**, *118*, 9772.

(20) (a) Fendrick, C. M.; Marks, T. J. *J. Am. Chem. Soc.* **1986**, *108*, 425. (b) Bruno, J. W.; Marks, T. J.; Morss, L. R. *J. Am. Chem. Soc.* **1983**, *105*, 6824.

and **3**, respectively, suggesting that the level of theory used is appropriate. Examining the TS structure, we find that it is a typical 4-center transition state commonly observed in σ-bond metathesis mediated by d^0 early transition metal and rare-earth metal systems.[21] In the transition state, there is a strong interaction between Ta and the migrating H atom, suggesting that the metal center plays an important role in the abstraction process. This is a result of 4-center−4-electron bonding interaction.[21]

As mentioned above, NMR spectra reveal a Berry pseudorotation process in **1**. One may wonder if it is possible for a pathway having the γ-H abstraction with an equatorial $-N(SiMe_3)_2$ ligand. Our model calculations showed that the activation free energy for such a pathway was 50.0 kcal/mol, significantly higher than that for the pathway discussed above. The reason for having such a high barrier is explained as follows. With the complex having the $-N(SiMe_3)_2$ ligand in the equatorial plane, the γ-H abstraction occurs through a transition state structure in which the metal center cannot have an interaction with the migrating H atom due to the small angle formed between the equatorial $-N(SiMe_3)_2$ and axial silyl ligands. In other words, the metal center does not play a role in stabilizing the transition state in such a pathway. Therefore, the corresponding transition state structure is highly unstable.

It should be noted that in our calculations SiH_3 is used to model the $-SiMe_3$ ligand. One may question whether the agostic feature of the $SiMe_3$ ligand is well modeled. We did a testing calculation on a model by replacing SiH_3 with $SiMe_3$ in **A**. The $SiMe_3$ model calculated does not differ much from **A**. Except for a slightly longer Ta−Si bond (2.805 Å in comparison to 2.759 Å in **A**), the differences for all other bonds are within 0.01 Å. The distances between Ta and β-H atoms in the $SiMe_3$ model calculated are greater than 3.9 Å. Clearly, no agostic C−H interactions can be found in the Ta−$SiMe_3$ moiety. The strong Ta−N π interactions probably prevent the formation of the agostic C−H bonds in these complexes. Although there are no clear signs of agostic C−H interactions in the Ta−$SiMe_3$ moiety, agostic $Si_\beta-C_\gamma$ interactions in the $Ta-N(SiMe_3)_2$ moieties exist in the crystal structure of **1**, as mentioned above. In the calculated model complex **A** where the disilylamide ligand was modeled by $N(SiH_3)(SiH_2Me)$, close contacts can be found between Ta and the $Si_\beta-C_\gamma$ bond. The $Ta\cdots C_\gamma$ and $Ta\cdots Si_\beta$ distances calculated for **A** are 3.68 and 3.40 Å, respectively, comparable to the experimental findings, although they are slightly longer due to the model ligands used in the gas-phase structure calculations.

(21) (a) Deelman, B.-J.; Teuben, J. H.; Macgergor, S. A.; Eisenstein, O. *New J. Chem.* **1995**, *19*, 691. (b) Ziegler, T.; Folga, E.; Berces, A. *J. Am. Chem. Soc.* **1993**, *115*, 636. (c) Floga, E.; Ziegler, T. *Can. J. Chem.* **1992**, *70*, 333.

Summary

In the current work, new Zr, Hf, and Ta silyl complexes were prepared and novel reactions of silyl ligands, γ-H abstraction to give a metallaheterocyclic moiety, were investigated. An analytical, kinetic formula for consecutive reactions involving an initial second-order reaction followed by a first-order reaction is derived. This new analytical method and a numerical method were used in this work to study the kinetics of the formation of the silyl complex **2a** and then its first-order γ-H abstraction to give metallacyclic complex **4a**. The γ-H abstraction reaction of Ta silyl complex **1** to give **3** was found to follow first-order kinetics with $\Delta H^{\ddagger} = 23.6(1.6)$ kcal/mol and $\Delta S^{\ddagger} = 3(5)$ eu between 288 and 313 K. The theoretical calculations here show that formation of the metallacyclic complexes through γ-H abstraction is entropically driven. The transition state for the γ-H abstraction is a 4-center TS, similar to those commonly observed in σ-bond metathesis of other d^0 metal systems.

Acknowledgment. This work was supported by the National Science Foundation (Grant CHE-0212137 to Z.-L.X) and Research Grants Council of Hong Kong and the Hong Kong University of Science and Technology (Grant HKUST6087/02P to Z.L.). We thank Profs. Xiaobing Feng, Forrest E. Michael, and T. Ffrancon Williams for helpful discussions.

Supporting Information Available: Details of kinetic calculations, plots of ln [**1**]/[**1**]$_0$ vs t and 1/[**6**] vs t, and listings of crystallographic data and Cartesian coordinates of all calculated structures in CIF format. This material is available free of charge via the Internet at http://pubs.acs.org.

IC049023V